Turkish Journal of Chemistry

http://journals.tubitak.gov.tr/chem/

Research Article

Turk J Chem
(2020) 44: 1327-1338
© TÜBİTAK
doi:10.3906/kim-2003-42

Preparation of different thin film catalysts by direct current magnetron sputtering for hydrogen generation

Gamze BOZKURT[1,*], Abdulkadir ÖZER[2], Ayşe BAYRAKÇEKEN YURTCAN[2,3]

[1]Project Coordination Implementation and Research Center, Erzurum Technical University, Erzurum, Turkey

[2]Chemical Engineering Department, Faculty of Engineering, Atatürk University, Erzurum, Turkey

[3]Nanoscience and Nanoengineering Department, Graduate School of Natural and Applied Sciences, Atatürk University, Erzurum, Turkey

Received: 20.03.2020 • **Accepted/Published Online:** 17.07.2020 • **Final Version:** 26.10.2020

Abstract: In this study, thin films of Co, Ni, Pd, and Pt were prepared on Co_3O_4 support material in pellet form using the direct current (DC) magnetron sputtering method for use as catalysts for hydrogen generation from $NaBH_4$.Characterization of the catalysts was carried out using X-ray diffraction (XRD), scanning electronic microscopy (SEM), and X-ray photoelectron spectroscopy (XPS). According to cross-sectional SEM images, catalyst thicknesses were observed in the range of approximately 115.3–495.8 nm. The particle sizes were approximately 25.0, 21.4, 33.9, and 9.5 nm for Ni-Co_3O_4, Co-Co_3O_4, Pd-Co_3O_4, and Pt-Co_3O_4 catalysts, respectively. The increase in NaOH initial concentration provides an increase in the rate of hydrogen generation for Co, Ni, and Pd catalysts. A maximum hydrogen generation rate of 1653 mL/g_{cat}.min was obtained for the Pt-Co_3O_4 catalyst.

Key words: Direct current magnetron sputtering, hydrogen generation, sodium borohydride, catalyst

1. Introduction

The reduction of greenhouse gas emissions worldwide and the use of alternative fuels in transportation have become a forced option. According to recent research, hydrogen is an innovative fuel option for the automotive field and could replace conventional petroleum-derived liquid mixtures in passenger cars over time. However, the generation and storage of hydrogen are important issues arising from the use of hydrogen energy. Compared to physical hydrogen storage methods, chemical hydrides have superior properties for hydrogen generation. Sodium borohydride ($NaBH_4$), which is a hydrogen storage material suitable for hydrogen generation, is the most remarkable chemical hydride due to its high hydrogen content and adjustable hydrogen release properties [1–11]. In the alkaline solution of $NaBH_4$ the catalysts act as an on/off switch to provide hydrogen release [2]. This situation enables hydrogen production at the desired time. The catalytic hydrolysis reaction of $NaBH_4$ is as follows:

$$NaBH_4 + (2 + x)\, H_2O \xrightarrow{catalyst} NaBO_2.xH_2O + 4H_2 + heat \quad (1)$$

A wide variety of catalysts are used for the hydrolysis of $NaBH_4$. Supported thin film catalysts are more easily recoverable than powder catalysts, and they do not aggregate [12]. Various methods enabling effective thin film catalysts such as pulsed laser deposition (PLD), electroplating, electroless plating, induced chemical reduction, and dip coating are used to obtain supported catalysts [13–17]. In addition to these methods, the direct current (DC) magnetron sputtering method can be used for thin film catalyst production. Because of its homogeneous wide area coating, good reproducibility, and high deposition rate, the DC magnetron sputtering method is the most attractive for industrial development [18]. The catalysts prepared by the sputtering method are deposited with precise control onto the support materials as thin, compact catalytic films, and because this low-cost method does not require precursors, the emission of toxic by-products is avoided. Film composition, structure, and morphology can be changed by varying sputtering parameters such as power, inert or reactive gas flow, partial pressure, and distance between the target and surface. A DC sputtering system is used for the coating of conductive materials, while a radio frequency (RF) sputtering system is used for nonconductive materials. When the uppermost layer needs to be active for catalysts, it is unnecessary for the metal to penetrate deeply into the substrate, and catalysts can be prepared more easily by DC sputtering[12,19]. Furthermore, DC sputtering is the cheapest method

* Correspondence: g13bozkurt@gmail.com

because DC power supplies are simpler to manufacture than those used in RF. In the magnetron process, in addition to an electrical field for acceleration of ionized argon atoms, a magnetic field is applied perpendicular to this field. By means of the magnetic field, electrons move along the helical orbit and, thus, increase the ion concentration on the target [20].

Very few studies have reported on catalysts for hydrolysis of $NaBH_4$ prepared by the sputtering method. In a study by Arzac et al., a cobalt catalyst was prepared on nickel foam by a magnetron sputtering method. They compared the hydrogen generation rates of catalysts having different film thicknesses and coated for different durations for sodium borohydride and ammonia boron hydrolysis. They reported that the highest activity for hydrogen generation from sodium borohydride was obtained from the catalyst coated for 4 h [12]. In addition, Co-based thin film catalysts are generally prepared by the different coating methods mentioned above. Therefore, the preparation of different thin film catalysts using the sputtering method for the hydrolysis reaction of $NaBH_4$ is an important working area.

In this study, Co_3O_4 synthesized in powder form was pelletized and coated separately with Ni, Co, Pd, and Pt metals via a DC magnetron sputtering technique applied for 20 min. The prepared catalysts were characterized by XRD, XPS, and SEM-EDS techniques. Afterwards, hydrogen generation and measurement experiments were carried out with a system designed by our group [21].

2. Experimental details

2.1. Synthesis of support material

Cobalt (II,III) oxide (Co_3O_4) powder support material was prepared by a chemical method as previously reported [22]. The Co_3O_4 synthesized in powder form was then pelletized by applying 10 tons of pressure with a manual press. The diameter and the thickness of the pellets were 13 mm and 0.2 mm, respectively. Pellets were then coated with Ni, Co, Pd, and Pt using the DC magnetron sputtering method.

2.2. Catalyst preparation with coating deposition

The catalysts were coated using a DC magnetron sputtering system (GSL-1100X-SPC-16M), and the conditions of the coating are given in Table 1. The distance between the substrate and the target was 40 mm, and targets with a diameter of 50.8 mm (Evochem and Quorum technologies, Ontario, Canada; 99.95% pure, 0.1–3mm thick) were used for sputtering. A mass flow controller was used to generate Ar gas flow into the chamber. The coating pressure of the vacuum level was maintained at $2.0–4.0\times10^{-2}$ Mbar, and current of 20 mA was applied for 20 min which led to the formation of plasma.

2.3. Characterization

The preparedcatalysts were examined by X-raydiffraction (XRD) using a PANalytical Empyrean X-ray diffractometer. The surface and cross-sectional morphology were examined by Quanta FEG 250 scanning electron microscope (SEM), and elemental composition of the coatings was determined by energy-dispersive X-ray spectrometry (EDS).The surface electronic states of the coated Ni, Co, Pd, and Pt metals were analysed by X-ray photoelectron spectroscopy (XPS) using the Specs-Flex X-ray photoelectron spectrometer.

2.4. Measurement of hydrogen generation rate

The activities of the catalysts were evaluated using a system designed by our group, as previously reported [21–22]. In all experiments, the effects of NaOH (99.99% pure) concentrations were investigated by stabilizing 10 wt% $NaBH_4$ (98% pure) solution with different initial concentrations of NaOH(1, 10 wt%) at 25 °C.

Table 1. The coating condition of DC magnetron sputtering.

Parameters	**Coating Conditions**
Equipment	DC Sputtering
Target	Ni, Co, Pd, Pt (99.99%)
Base pressure	10^{-2} mbar
Working pressure	$4x10^{-2}$ mbar
Gas	Argon
Deposition time	20 min
Power supply	AC 110V 60Hz
Applied current	20 mA

3. Results and discussion

3.1. Characterization of the catalysts

The XRD patterns of the Co-Co_3O_4, Ni-Co_3O_4,Pd-Co_3O_4, and Pt-Co_3O_4 catalysts, which were compared with the diffraction pattern of Co_3O_4, are shown in Figure 1. According to the XRD results, $Co_3O_4$with a polycrystalline cubic structure was obtained. Characteristic peaks of Ni corresponding to (111) and (200) planes for 2Θ values of 44.5 and 55.8° may overlap with the (400) and (422) planes of Co_3O_4, respectively; (002) and (101) plane peaks were observed for Co. Three diffraction peaks corresponding to the (111), (200), and (220) planes for 2Θ values of 40.4, 46.9, and 68.6° were observed for Pd. In addition, the three peaks detected for Pt were assigned to diffraction from the (111), (200), and (220) planes for 2Θ values of 39.6, 45.4, and 70°, respectively. The grain sizes of the prepared catalysts were calculated from the XRD data using the Scherrer equation [23]. The grain sizes were approximately 25.0, 21.4, 33.9, and 9.5 nm for Ni-Co_3O_4, Co-Co_3O_4, Pd-Co_3O_4, and Pt-Co_3O_4 catalysts, respectively. The (111) planes at around 2Θ value of 45° were selected to calculate the grain sizes of Ni and Co catalysts. Similarly, the (111) planes at around 2Θ value of 40° were selected to calculate the grain size of Pd and Pt catalysts.

The SEM image given in Figure 2a shows surface morphologies (particle nature) for the Co_3O_4 support material in pellet form. Particle formation with homogeneous dispersion was observed in Co_3O_4 support material, according to the EDS analysis given for Co_3O_4 in Figure 2b. In addition, Figure 2c shows the prepared Co_3O_4 pellet.

Figures 3–6 show SEM images of prepared catalysts from both the surface and cross sectional areas as well as the EDS results for the catalysts.

Figures 3a–c show the surface and cross sectional SEM images and EDS analysis of Co-Co_3O_4. According to Figure 3a, particle formation was observed with nonhomogeneous dispersion for Co-Co_3O_4. The Co layer thickness was clearly observed from the cross sectional SEM images of the catalyst (Figure 3b). Catalyst thickness was approximately 115.3 nm. According to the EDS spectrum (Figure 3c), Co and O elements were detected for the catalyst.

Figures 4a–c show the surface and cross sectional SEM images and EDS analysis of Ni-Co_3O_4. According to Figure 4a, particle formation was observed with nonhomogeneous dispersion for Ni-Co_3O_4. The Ni layer thickness was clearly observed from the cross sectional SEM images of the catalyst (Figure 4b). Catalyst thickness was approximately 267.4 nm. According to the EDS spectrum(Figure4c) Ni, Co, and O elements were detected for the catalyst. A low nickel-coating ratio was observed in this case.

Figures 5a–c show the surface and cross sectional SEM images and EDS analysis of Pd-Co_3O_4.According to Figure5a, particle formation had homogeneous dispersion compared to Co- and Ni-based catalysts for Pd-Co_3O_4. In addition, the Pd

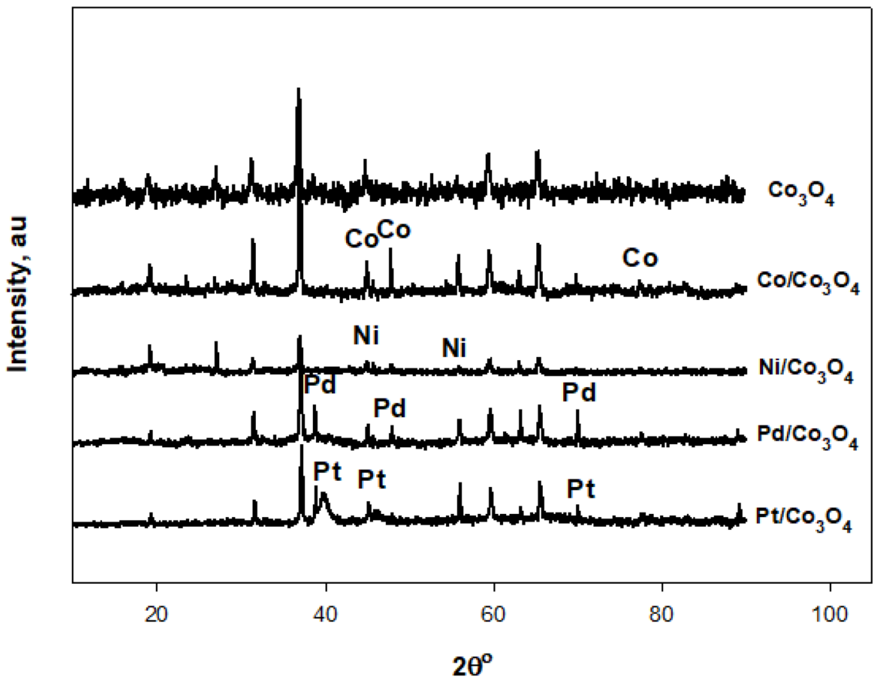

Figure 1. XRD patterns of the support material and catalysts.

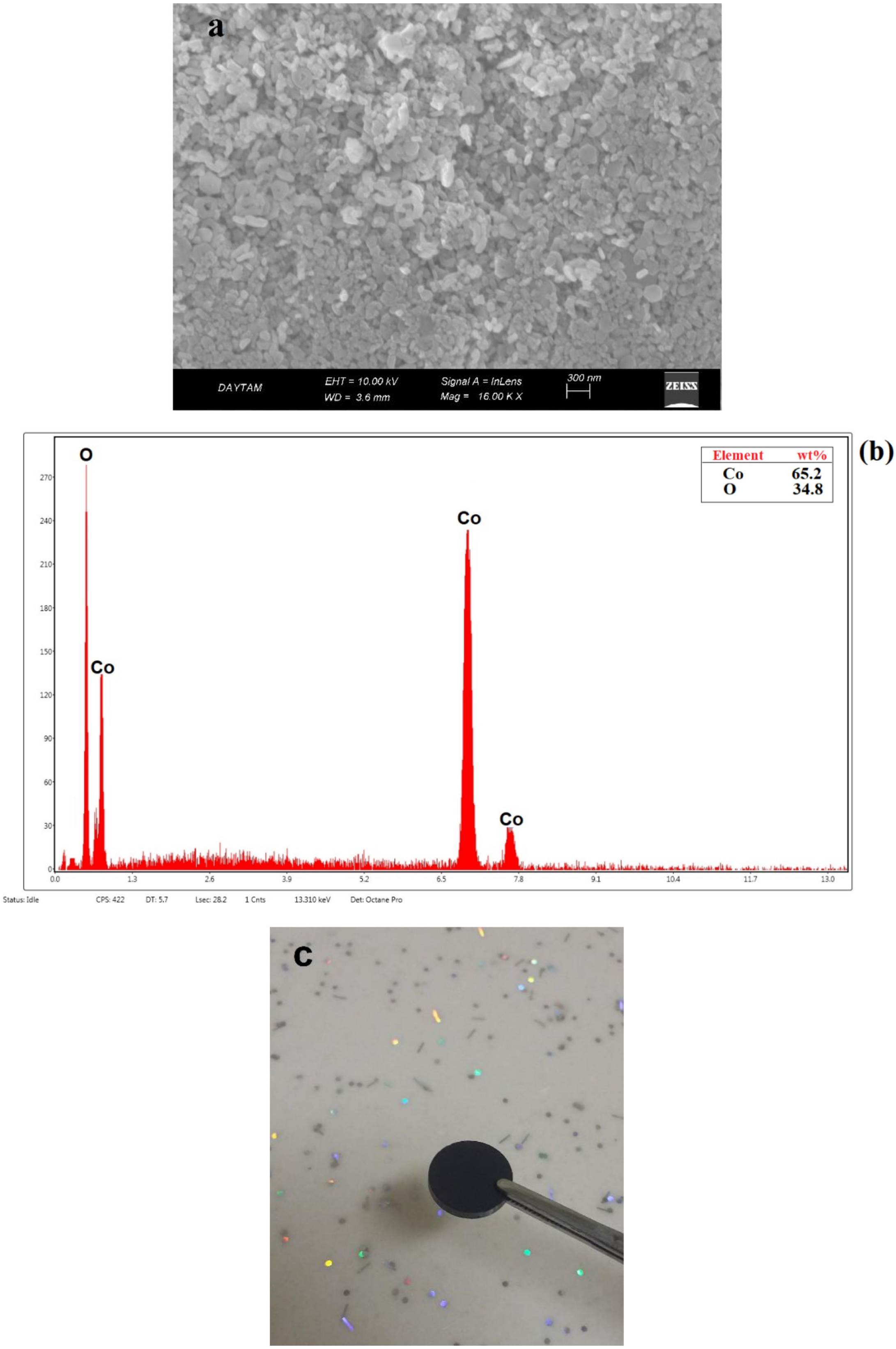

Figure 2. a) SEM image b) EDS analysis c) photo for Co_3O_4 pellet.

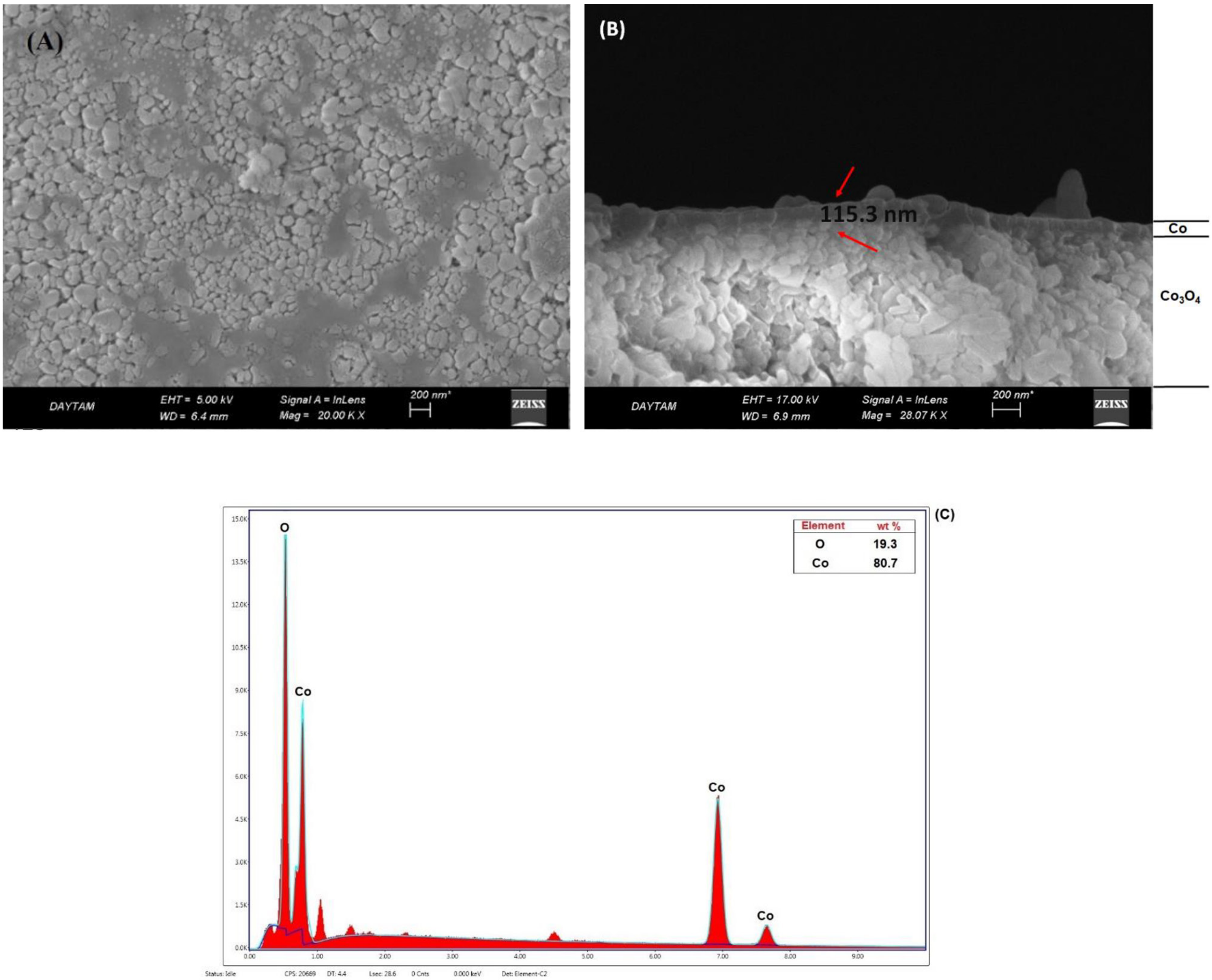

Figure 3. A) Surface B) cross sectional SEM images, and C) EDS analysis result for Co-Co_3O_4 catalyst.

particle sizes were larger than Ni and Co particles. This confirms the average particle size results calculated for the catalysts using XRD data. The Pd layer thickness was clearly observed from cross sectional SEM images of the catalyst (Figure 5b). Catalyst thickness was approximately 495.8 nm. According to the EDS spectrum (Figure 5c) Pd, Co, and O elements were detected for the catalyst, and a severe peak of Pd was observed.

Figures 6a–c show the surface and cross sectional SEM images and EDS analysis of Pt-Co_3O_4. Homogeneous particle formation was observed for Pt-Co_3O_4 catalyst, similar to the Pd-Co_3O_4 catalyst (Figure 6a). The Pt layer thickness was clearly observed from the cross sectional SEM images of the catalyst (Figure 6b). Catalyst thickness was approximately 285.5 nm. According to the EDS spectrum (Figure 6c), Pt, Co, and O elements were detected for the catalyst, and a severe peak of Pt was observed.

Figure 7 illustrates the XPS spectra of general and Co 2p, Ni 2p, Pd 3d, and Pt 4d–4f level photoemission signals of the catalysts. Figures 7a, 7c, 7e, and 7g show the XPS spectra of general elements. According to Figure 7b, two prominent peaks were observed for Co $2p_{3/2}$ and Co $2p_{1/2}$ (779.6 eV and 795.5 eV, respectively). Two shake-up satellites at 802.8 and 787.2 eV indicate the presence of Co_3O_4 [24]. Two peaks of $2p_{3/2}$ and $2p_{1/2}$ for Ni were observed at 852.7 and 870.6 eV, respectively (Figure 7d) [25]. Figure 7f shows 334.5 eV($3d_{5/2}$) and 338.8 eV($3d_{3/2}$) corresponding to the Pd metal and Pd^{+2}states, respectively [26]. The peaks located at binding energies of 316.3 and 333.2 eV (Figure 7h) can be attributed to the Pt $4d_{5/2}$ and Pt $4d_{3/2}$ regions, respectively [27].Furthermore, Figure 7i shows Pt $4f_{7/2}$ and Pt $4f_{5/2}$ peaks, demonstrating the reduction of Pt(IV) to Pt(0) [28].

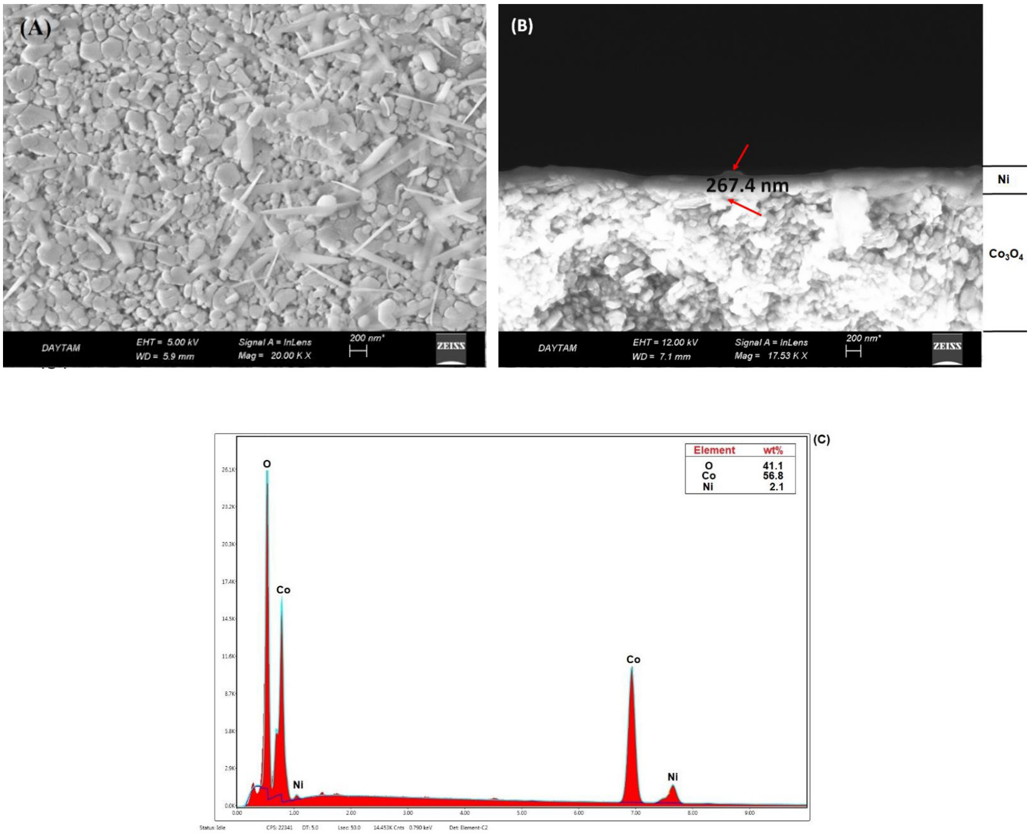

Figure 4. A) Surface B) cross sectional SEM images, and C) EDS analysis result for Ni-Co_3O_4 catalyst.

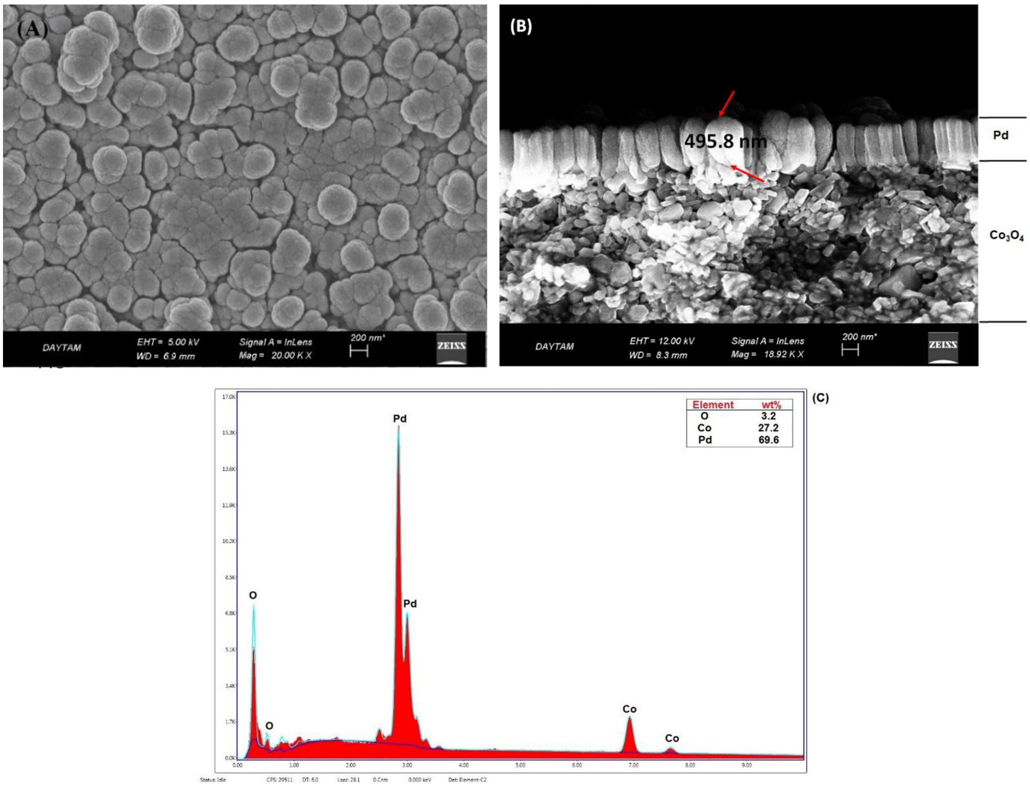

Figure 5. A)Surface B) cross sectional SEM images, and C) EDS analysis result for Pd-Co_3O_4 catalyst.

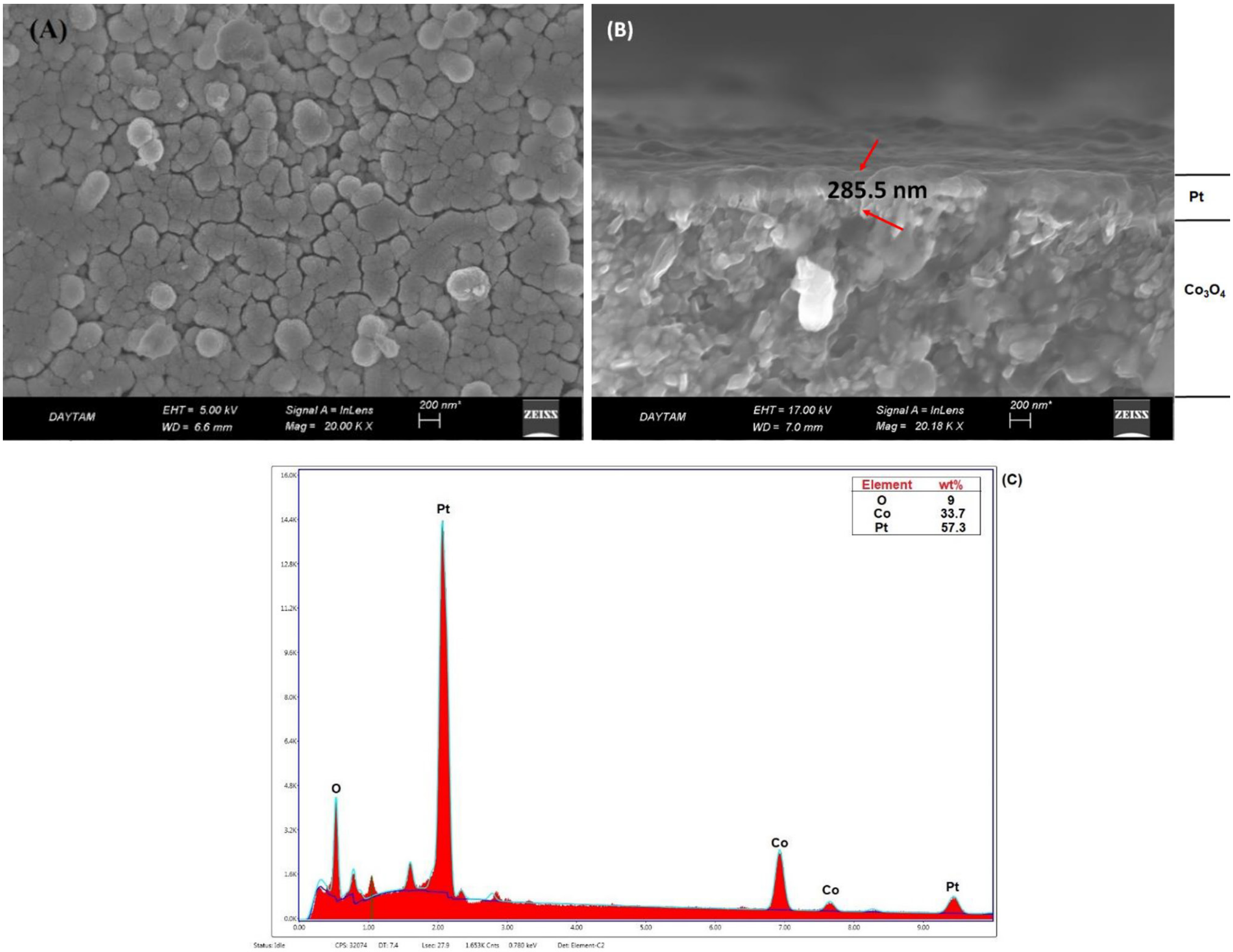

Figure 6. A) Surface B) cross sectional SEM images, and C) EDS analysis result for Pt-Co_3O_4 catalyst.

3.2. Hydrogen generation of the catalysts

Figures 8–11 show the amounts of hydrogen generated from $NaBH_4$ hydrolysis at 1 wt% and 10 wt% NaOH initial concentrations. All the experiments were performed at 25°C and 10 wt% $NaBH_4$. The hydrogen generation rates of the catalysts for 1% and 10%NaOH initial concentrations are given in Table 2. Increasing the initial NaOH concentration for Ni, Co, and Pd-Co_3O_4catalysts caused an increase in the hydrogen generation rate (Figures 8–10). This increase was more than 2.5 times for the Pd-Co_3O_4 catalyst. An increase in the hydrogen generation rate of the Pd-based catalyst following an increase in the NaOH initial concentration was observed in a previous study by our group and was attributed to inclusion of the hydroxyl ion in$NaBH_4$ hydrolysis [21]. Similarly, the increase in NaOH initial concentration for Ni- and Co-based catalysts had a positive effect [22].The Co-Co_3O_4 catalyst was the most active among the three catalysts. The hydrogen generation rate for the Co-Co_3O_4 catalyst at an initial concentration of 10% NaOH was 945 mL/g_{cat}.min. InRakap et al. the activity of a Co-Ni-P/Pd-TiO_2 catalyst prepared with an electroplating method was investigated at 25°C, and the hydrogen generation rate was 460 mL/g_{cat}.min [29]. Similarly, in a study by Krishnan et al., the hydrogen generation rate of a Co-B catalyst prepared on Ni foam was 300 mL/g_{cat}.min [30]. In contrast, when the initial concentration of NaOH for the Pt catalyst increased from 1% to 10%, a decrease in the hydrogen generation rate was observed (Figure 11). The highest hydrogen generation rate was obtained from the Pt-Co_3O_4 catalyst in 1% NaOH initial concentration (1653 mL/g_{cat}.min). At an initial concentration of 10% NaOH in the Pt-Co_3O_4 catalyst, the hydrogen generation rate decreased due to the reduced amount of free water required for the reaction and the low solubility of the reaction by-product $NaBO_2$ [21]. Hydrogen generation rates from the $NaBH_4$ hydrolysis of Ni-, Co-, Pd-, and Pt-based catalysts prepared in this work, and catalysts prepared using different thin film methods described in the literature, were compared in Table 3 [12–17, 29–33]. As shown in Table 3, hydrogen generation rates changed significantly depending on the catalysts used as well as the thin

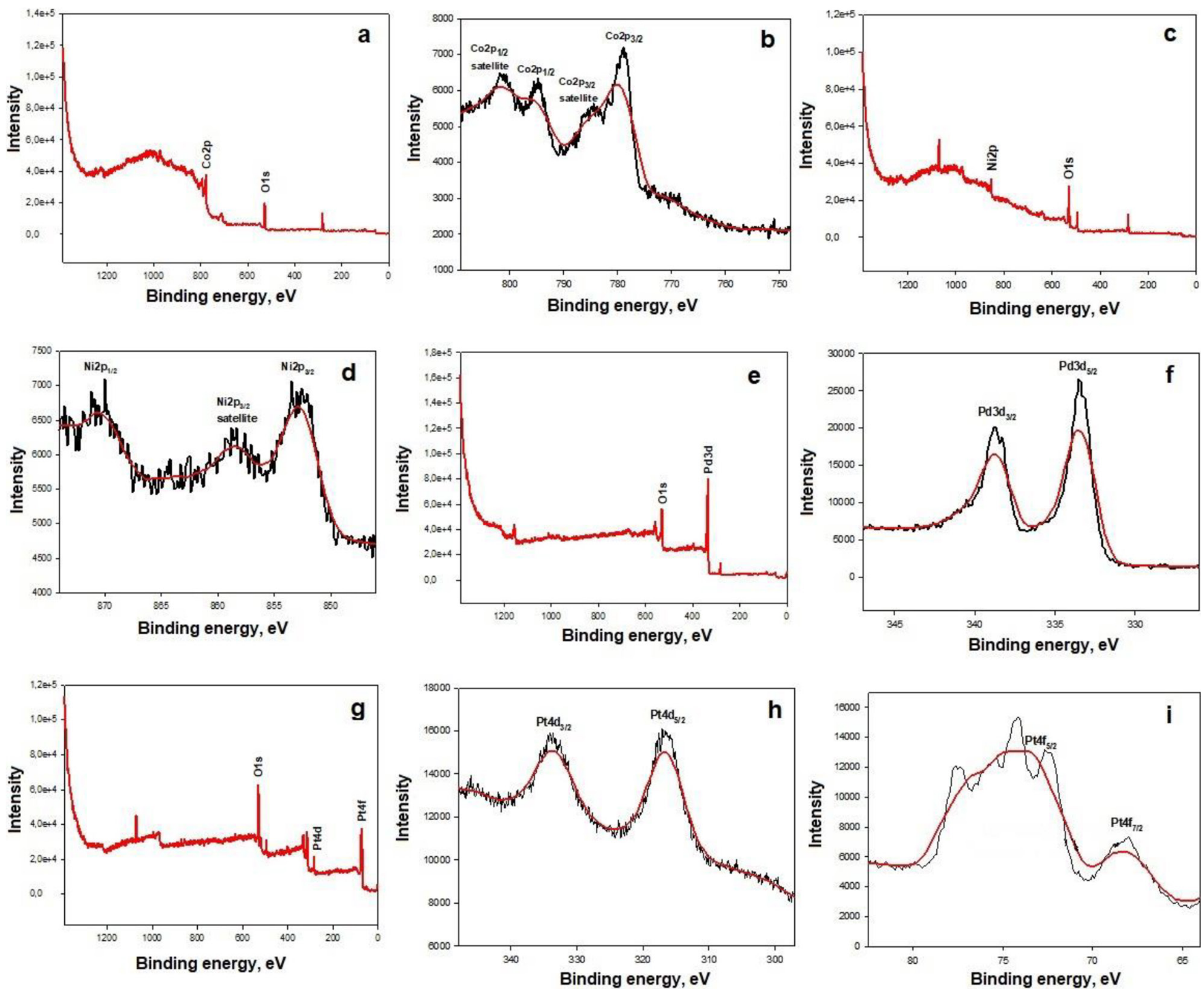

Figure 7. XPS spectrums for; Co-Co_3O_4 catalyst (a) general spectrum (b) Co 2p, Ni- Co_3O_4 catalyst (c) general spectrum (d) Ni 2p, Pd-Co_3O_4 catalyst (e) general spectrum (f) Pd 3, Pt- Co_3O_4 catalyst (g) general spectrum (h) Pt 4d (i) Pt 4f electron regions.

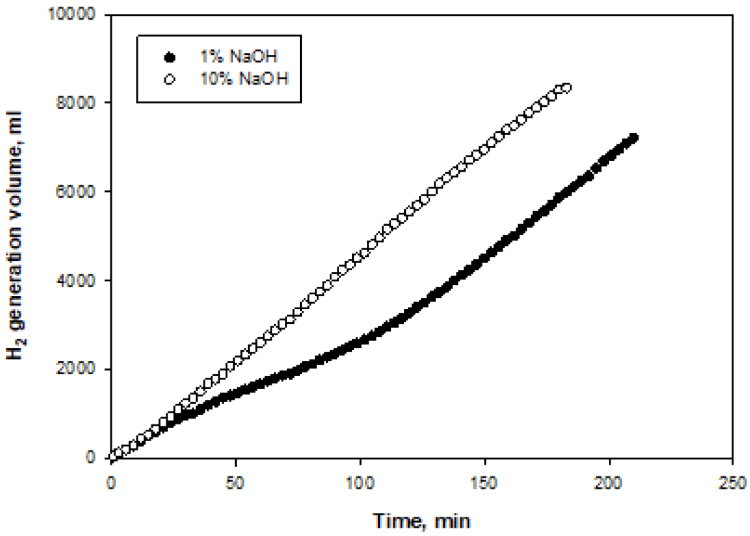

Figure 8. Time-dependent volumes of hydrogen generated at two different NaOH initial concentrations for Co-Co_3O_4 catalyst.

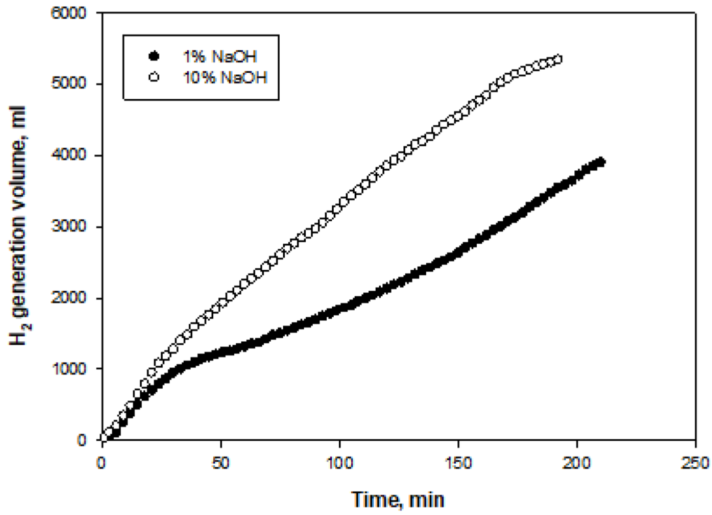

Figure 9. Time-dependent volumes of hydrogen generated at two different NaOH initial concentrations for Ni-Co_3O_4 catalyst.

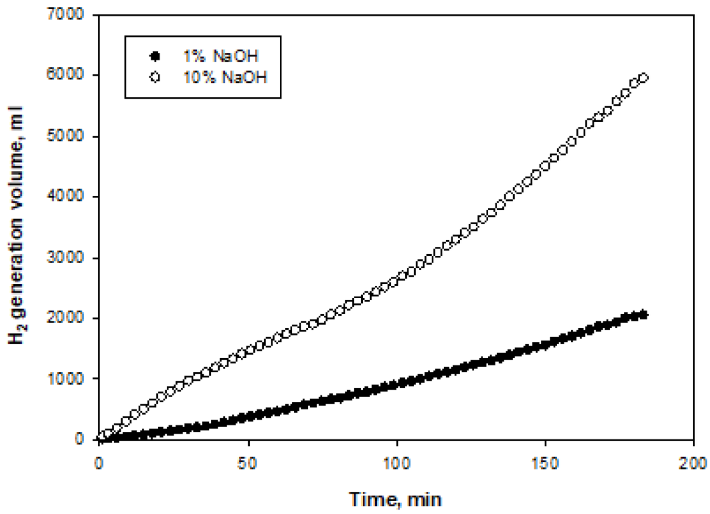

Figure 10. Time-dependent volumes of hydrogen generated at two different NaOH initial concentrations for Pd-Co_3O_4 catalyst.

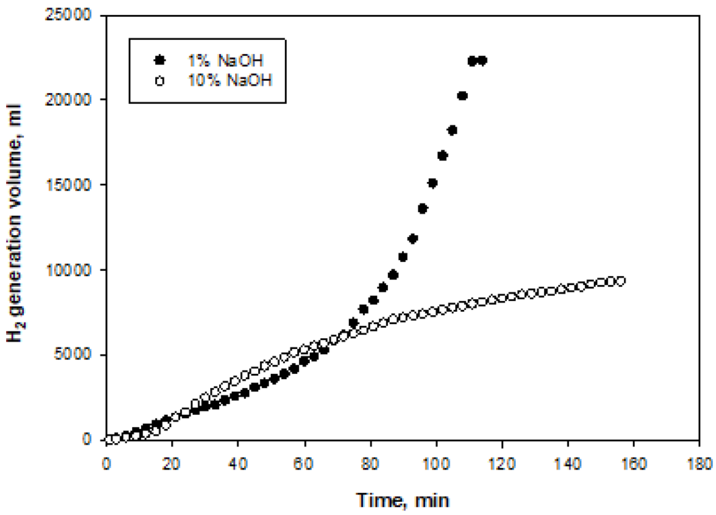

Figure 11. Time-dependent volumes of hydrogen generated at two different NaOH initial concentrations for Pt-Co_3O_4 catalyst.

Table 2. H_2 generation rate (HGR) of catalysts at two different NaOH initial concentrations.

Catalyst	HGR, ml/g_{cat}.min	
	1% NaOH	10% NaOH
Co-Co_3O_4	587	945
Ni-Co_3O_4	568	782
Pd-Co_3O_4	229	614
Pt-Co_3O_4	1653	1382

Table 3. HGRs for hydrolysis of $NaBH_4$ catalyzed by various catalysts in the literature.

Catalysts	Method	Operating conditions			HGR, ml/ g_{cat}.min	Film thickness, nm	Ref
		wt% $NaBH_4$	wt% NaOH	Temp. (^{o}C)			
Co-Ni-P/Pd-TiO_2	electroless plating	0.3 M	10	25	460	-------	[29]
Co-B/Ni foam	electroplating electroless plating	10	5	25	300 1640	10000-15000	[14]
Co-P/Cu	electroplating	10	1	30	954	Increase with an increase in duration	[30]
Co film/Cu foil	magnetic-field-induced chemical reduction	0.2 M	0.4 M	25	1270	-------	[16]
Co-P/Cu sheet	electroless plating	5	1	30	2275.1	-------	[15]
Co/Ni foam	magnetron sputtered	1M	4.5	25	2650	2000	[12]
Co–B/Pd	dry dip-coating	20	1M	30	2875	-------	[17]
Co-B/ silicon	PLD	1	5	room	3300	Particle sizes (180-300 nm)	[31]
Co–Ni–P/Cu	electroplating	10	10	25	3636	-------	[32]
Co–P–B	PLD	0.025 M	0.025 M	room	4230	-------	[13]
Co-W-P/Cu	electroplating	10	10	30	5000	-------	[33]
Pd-Co_3O_4 Ni-Co_3O_4 Co-Co_3O_4	DC magnetron sputtered	10	10	25	614 782 945	495.8 267.4 115.3	This work
Pt-Co_3O_4	DC magnetron sputtered	10	1	25	1653	285.5	This work
PLD: Pulsed laser deposition DC: direct current							

film preparation techniques. In this study, the efficiency of thin film catalysts prepared by the DC magnetron sputtering method for noble and nonnoble metals was investigated, and promising results were observed.

4. Conclusions

In this study, Ni, Co, Pd, and Pt metals supported by a Co_3O_4 pellet were prepared using a DC magnetron sputtering method for hydrogen generation from the hydrolysis of $NaBH_4$. The SEM images for the catalysts illustrated surface morphologies and cross sectional areas. The Pd and Pt particles have nearly uniform size, and good dispersions were obtained. Catalyst layer thicknesses were clearly observed at 115.3, 267.4, 495.8, and 285.5 nm for Co, Ni, Pd, and Pt, respectively. According to the XRD results, the highest particle size obtained from a Pd-based catalyst was approximately 33.9 nm. The hydrogen generation rates of the catalysts were investigated at 1% and 10% NaOH initial concentrations. An increase in the NaOH initial concentration provides an increase in the rate of hydrogen generation for Co, Ni, and Pd catalysts. The minimum hydrogen generation rates were observed with a Pd-based catalyst. The reason may be that the Pd-based catalyst has a higher average particle size and a higher catalyst thickness than other catalysts. The highest hydrogen generation rate was obtained from the Pt-Co_3O_4 catalyst in 1% NaOH initial concentration (1653 mL/g_{cat}.min).

Acknowledgments
The authors gratefully acknowledge a doctoral research scholarship from the Scientific and Technological Research Council of Turkey (TÜBİTAK) (grant no. 1649B031502644) as well as the financial support of the Atatürk University BAP Project (grant no. 2015/127).

References

1. Zabielaite A, Balciunaite A, Stalnioniene I, Lichusina S, Simkunaite Detal. Fiber-shaped Co modified with Au and Pt crystallites for enhanced hydrogen generation from sodium borohydride. International Journal of Hydrogen Energy 2018; 43: 23310-23318. doi: 10.1016/j.ijhydene.2018.10.179

2. Wang J, Ke D, Li Y, Zhang H, Wang C et al. Efficient hydrolysis of alkaline sodium borohydride catalyzed by cobalt nanoparticles supported on three–dimensional graphene oxide. Materials Research Bulletin 2017; 95: 204-210. doi: 10.1016/j.materresbull.2017.07.039

3. Zhang X, Sun X, Xu D, Tao X, Dai P et al. Synthesis of MOF-derived Co@C composites and application for efficient hydrolysis of sodium borohydride. Applied Surface Science 2019; 469: 764-769.doi: 10.1016/j.apsusc.2018.11.094

4. Huang ZM, Su A, Liu YC. Hydrogen generation with sodium borohydride solution by Ru catalyst. International Journal of Energy Research 2013; 37: 1187-1195.doi: 10.1002/er.2937

5. Inokawa H, Driss H, Trovela F, Miyaoka H, Ichikawa Tet al. Catalytic hydrolysis of sodium borohydride on Co catalysts. International Journal of Energy Research 2016; 40: 2078-2090. doi: 10.1002/er.3582

6. Chen Y, Liu L, Wang Y, Kim H. Preparation of porous PVDF-NiB capsules as catalytic adsorbents for hydrogen generation from sodium borohydride. Fuel Processing Technology 2011; 92: 1368-1373.doi: 10.1016/j.fuproc.2011.02.019

7. Chen Y, Kim H. Use of a nickel-boride–silica nanocomposite catalyst prepared by in-situ reduction for hydrogen production from hydrolysis of sodium borohydride. Fuel Processing Technology 2008; 89: 966-972. doi: 10.1016/j.fuproc.2008.04.005

8. Cai H, Lu P, Dong J. Robust nickel–polymer nanocomposite particles for hydrogen generation from sodium borohydride. Fuel 2016; 166: 297-301.doi: 10.1016/j.fuel.2015.11.011

9. Sahin Ö, Dolas H, Kaya M, Izgi MS, Demir H. Hydrogen production from sodium borohydride for fuel cells in presence of electrical field. International Journal of Energy Research 2010; 34: 557–567. doi: 10.1002/er.1563

10. Sahiner N, Seven F. A facile synthesis route to improve the catalytic activity of inherently cationic and magnetic catalyst systems for hydrogen generation from sodium borohydride hydrolysis. Fuel Processing Technology 2015; 132: 1-8. doi: 10.1016/j.fuproc.2014.12.008

11. Chen Y, Shi Y, Liu X, Zhang Y. Preparation of polyvinylidene fluoride–nickel hollow fiber catalytic membranes for hydrogen generation from sodium borohydride. Fuel 2015; 140: 685-692. doi: 10.1016/j.fuel.2014.10.022

12. Paladini M, Arzac GM, Godinho V, Haro MCJD, Fernandez A. Supported Co catalysts prepared as thin films by magnetron sputtering for sodium borohydride and ammonia borane hydrolysis.Applied Catalysis B: Environmental 2014; 158-159: 400-409. doi: 10.1016/j.apcatb.2014.04.047

13. Patel N, Fernandes R, Bazzanella N, Miotello A. Co–P–B catalyst thin films prepared by electroless and pulsed laser deposition for hydrogen generation by hydrolysis of alkaline sodium borohydride: A comparison. Thin Solid Films2010; 518: 4779-4785.doi: 10.1016/j.tsf.2010.01.029

14. Krishnan P, Advani SG, Prasad AK. Thin-film CoB catalyst templates for the hydrolysis of $NaBH_4$ solution for hydrogen generation, Applied Catalysis B: Environmental 2009; 86:137-144. doi: 10.1016/j.apcatb.2008.08.005

15. Wang Y, Shen Y, Qi K, Cao Z, Zhang K et al. Nanostructured cobalt–phosphorous catalysts for hydrogen generation from hydrolysis of sodium borohydride solution. Renewable Energy 2016; 89: 285-294. doi: doi.org/10.1016/j.renene.2015.12.026

16. Li H, Liao J, Zhang X, Liao W, Wen L et al. Controlled synthesis of nanostructured Co film catalysts with high performance for hydrogen generation from sodium borohydride solution. Journal of Power Sources 2013; 239: 277-283. doi: 10.1016/j.jpowsour.2013.03.167

17. Liang J, Li Y, Huang Y, Yang J, Tang H et al. Sodium borohydride hydrolysis on highly efficient Co–B/Pd catalysts. International Journal of Hydrogen Energy 2008; 33: 4048-4054. doi: 10.1016/j.ijhydene.2008.05.082

18. Kim SI, Cho SH, Choi SR, Yoon HH, Song PK. Properties of ITO films deposited by RF superimposed DC magnetron sputtering. Current Applied Physics 2009; 9: S262-S265.doi: 10.1016/j.cap.2009.01.031

19. Guizard C, Princivalle A. Preparation and characterization of catalyst thin films. Catalysis Today 2009; 146: 367-377. doi: 10.1016/j.cattod.2009.05.012

20. Wasa K, Hayakawa S. Handbook of Sputter Deposition Technology. 1th ed. New Jersey, ABD: Noyes;1992.

21. Bozkurt G, Özer A, Yurtcan AB. Development of effective catalysts for hydrogen generation from sodium borohydride: Ru, Pt, Pd nanoparticles supported on Co_3O_4. Energy 2019; 180: 702-713. doi: 10.1016/j.energy.2019.04.196

22. Bozkurt G, Özer A, Yurtcan AB. Hydrogen generation from sodium borohydride with Ni and Co based catalysts supported on Co_3O_4. International Journal of Hydrogen Energy 2018; 43: 22205-22214. doi: 10.1016/j.ijhydene.2018.10.106

23. Patterson AL. The Scherrer Formula for X-Ray Particle Size Determination. Physical Review 1939; 56: 978-982. doi: 10.1103/PhysRev.56.978

24. Kuang M, Li TT, Chen H, Zhang SM, Zhang LL et al. Hierarchical Cu_2O/CuO/Co_3O_4 core-shell nanowires: synthesis and electrochemical properties. Nanotechnology 2015; 26: 304002-304010. doi:10.1088/0957-4484/26/30/304002

25. Wang X, Yu H, Yang L, Shao L, Xu L. A highly efficient and noble metal-free photocatalytic system using NixB/CdS as photocatalyst for visible light H_2 production from aqueous solution. Catalysis Communications 2015; 67: 45-48. doi: 10.1016/j.catcom.2015.03.026

26. Smith EF, Garcia IJ, Briggs D, Licence P. Ionic liquids in vacuo; solution-phase X-ray photoelectron spectroscopy. Chemical Communications 2005; 45: 5633-5635. doi:10.1039/B512311A

27. Pana O, Leostean C, Soran ML, Stefan M, Macavei Set al. Synthesis and characterization of Fe–Pt based multishell magnetic nanoparticles. Journal of Alloys and Compounds 2013; 574: 477-485. doi: 10.1016/j.jallcom.2013.05.153

28. Benaissi K, Johnson L, Walsh DA, Thielemans W. Synthesis of platinum nanoparticles using cellulosic reducing agents. Green Chemistry 2010; 12: 220-222. doi: 10.1039/B913218J

29. Rakap M, Kalu EE, Özkar S. Cobalt–nickel–phosphorus supported on Pd-activated TiO_2 (Co–Ni–P/Pd-TiO_2) as cost-effective and reusable catalyst for hydrogen generation from hydrolysis of alkaline sodium borohydride solution.Journal of Alloys and Compounds 2011; 509: 7016-7021. doi: 10.1016/j.jallcom.2011.04.023

30. Cho KW, Kwon HS. Effects of electrodeposited Co and Co–P catalysts on the hydrogen generation properties from hydrolysis of alkaline sodium borohydride solution.Catalysis Today 2007; 120: 298-304. doi: 10.1016/j.cattod.2006.09.004

31. Patel N, Guella G, Kale A, Miotello A, Patton Bet al. Thin films of Co–B prepared by pulsed laser deposition as efficient catalysts in hydrogen producing reactions.Applied Catalysis A: General 2007; 323: 18-24. doi: 10.1016/j.apcata.2007.01.053

32. Guo Y, Feng Q, Ma J. The hydrogen generation from alkaline $NaBH_4$ solution by using electroplated amorphous Co–Ni–P film catalysts. Applied Surface Science 2013; 273: 253-256. doi: 10.1016/j.apsusc.2013.02.025

33. Guo Y, Dong Z, Cui Z, Zhang X, Ma J. Promoting effect of W doped in electrodeposited Co–P catalysts for hydrogen generation from alkaline $NaBH_4$ solution. International Journal of Hydrogen Energy 2012; 37: 1577-1583. doi: 10.1016/j.ijhydene.2011.10.019